DETECTION LIMIT OF XRF MEASUREMENTS AT DIFFERENT SYNCHROTRON RADIATION FACILITIES

A. Zuschlag, G. Hahn
University of Konstanz, Department of Physics, P.O. Box X916, 78457 Konstanz, Germany
Author for correspondence: annika.zuschlag@uni-konstanz.de, Tel.: +49 7531 88 3174, Fax: +49 7531 88 3895

ABSTRACT: The only possibility to determine the spatial distribution of transition metal precipitates in silicon wafers without destroying the sample is X-Ray Fluorescence (XRF). The purpose of this work is to evaluate the measurement conditions at different synchrotron radiation facilities. Therefore, we prepared metal test structures with different sizes on the surface of a FZ silicon wafer by electron beam lithography. The investigation of metal particles with a known size and distribution allows the determination of the detection limit at different beamline setups. The gained results are important for further experiments based on synchrotron radiation at different facilities and the evaluation of XRF results. This investigation leads also to an optimization of the measurement setup due to focusing on structures with known shape, which results in improved XRF measurement conditions.
Keywords: characterization, defects, evaluation

1 INTRODUCTION

The use of cost-effective silicon material usually goes along with a higher defect density in the silicon wafer. Besides other defects, the transition metal content in the silicon wafer influences the material quality and the solar cell performance, e.g. in [1]. Within a silicon wafer the transition metal content is the sum of transition metal precipitates and the interstitial metal concentration. The interstitial transition metal content is not directly detectable, only its influence on the minority carrier lifetime allows an evaluation of its distribution. In opposite, transition metal precipitates can be directly detected by XRF (X-Ray Fluorescence) measurement methods based on synchrotron radiation [2]. This is the only possibility to determine the spatial distribution of transition metal precipitates without destroying the sample. Several publications have shown the importance of XRF measurements for photovoltaic research. Examples are transition metal distribution in the wafer (e.g. [2]), influence of metal precipitates on recombination activity (e.g. [3]), precipitate dissolution kinetics (e.g. [4]) and their behaviour during standard solar cell processing steps [5-7] among other research topics. Besides XRF, other synchrotron radiation based measurement methods are used to determine the recombination activity (XBIC: X-ray Beam Induced Current) [8], the chemical state (XANES: X-ray Absorption Near Edge Spectroscopy) or micro-photoluminescence spectroscopy on metal precipitates in silicon (XEOL: X-ray Excited Optical Luminescence) [9].

All these measurement methods are very time consuming and allow only the investigation of small regions in the µm range. The access to synchrotron facilities is usually limited and a strict and a well planed operating schedule for XRF based experiments is needed. This includes the choice of a beamline which fits the required measurement conditions, like e.g. the detection limit. The detection limit may be critical especially for investigations on non contaminated silicon materials or on the influence of process treatments on the metal precipitates within a silicon wafer.

In this work we discuss the detection limit of XRF for three different synchrotron radiation facilities:

1) µSpot beamline at Berliner Elektronen-Speicherring für SYnchrotron-Strahlung (BESSY II) in Berlin, Germany,

2) beamline ID22N at the European Synchrotron Radiation Facility (ESRF) in Grenoble, France, and

3) beamline 2-ID-D at the Advanced Photon Source (APS) in Argonne, USA.

The measurement setup is different for these three beamlines (e.g. the focussing method) which results in different detection limits, applications and advantages.

2 EXPERIMENT

In case of XRF the sample moves relative to the incident beam while the fluorescence spectra are detected for each single point. The extraction of the characteristic fluorescence of an element results in a map of the spatial distribution of this material. The intensity of the measurement signal depends on the size of the metal precipitate and its depth within the wafer. The depth could be assumed by comparison of the K_α und K_β signal: their ratio is influenced by the different absorption coefficients for different wavelengths. Further on, the intensity of the fluorescence signal is influenced by the sum of all precipitates within a region covered by the X-ray beam spot which is usually larger than the observed precipitates. Therefore, small precipitates which are located closely together can result in the same fluorescence signal as a single larger precipitate. This complicates the interpretation of XRF results especially in case of measurements before and after process treatments to evaluate their impact on the distribution of transition metal precipitates.

To determine the detection limit of the different beamlines, transition metal structures on a sample with known distribution and sizes are essential. Therefore, samples with transition metal structures of different sizes on the surface were fabricated by electron beam lithography and analyzed by electron microscopy and atomic force microscope measurements.

3 SAMPLE PREPARATION

To evaluate the detection limit of several synchrotron radiation facilities, metallic test structures were fabricated on a polished silicon FZ wafer by electron beam lithography.

The samples were cleaned and covered with PMMA as E-beam resist by spin coating. After a bake-out process the samples were further processed by electron

beam writing. Besides the high spatial resolution, electron beam lithography has also the advantage that the design of the writing pattern can be easily adjusted to the needs of the different measurement setups of synchrotron facilities. This includes the adjustment of marking structures as well as the sizes and distances between the metal structures for µXRF investigations. After E-beam writing the samples were developed in MIBK:IPA, which results in an evaporation mask built by the remaining resist. Different metals like Cr and Cu were thermally evaporated on the samples. Afterwards, the E-beam resist as well as the metal layer on the resist were removed in acetone. The sizes of remaining metal structures on the silicon wafer were measured by scanning electron microscopy. The thickness of the metal structures has been determined by atomic force microscopy.

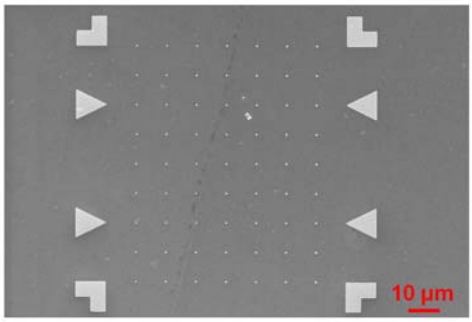

Figure 1: Scanning electron microscopy overview of chromium structures (markers and cylinders with different diameters) on a FZ-Si wafer, fabricated by E-beam lithography.

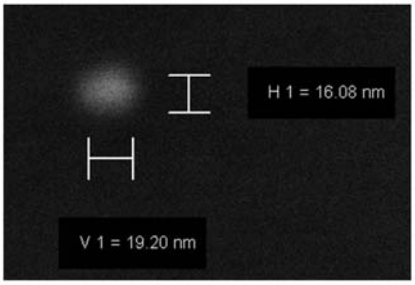

Figure 2: Scanning electron microscopy image of an exemplary single chromium structure on a FZ-Si wafer.

This electron beam lithography method leads to cylindric structures while their heights could be adjusted by metal evaporation. The smallest structure on a sample was 15 nm in diameter with a thickness of the metal layer in the range of 12 nm. This results in a volume which is equivalent to a sphere with a radius of 8 nm. Fig. 1 shows exemplary an electron microscopy image of a writing field including markers with 72 chromium structures of different sizes, while Fig. 2 shows exemplarily a single chromium cylinder with a radius of only a few nm.

4 EXPERIMENTAL RESULTS

Due to the different measurement setups at the beamlines of several synchrotron radiation facilities, the results for each beamline will be discussed separately.

BESSY II

First, results of the µSpot beamline at BESSY II in Berlin, Germany will be discussed. A capillary optic focuses the beam to a relatively large spot size of 3.5 µm (FWHM). The beam hits the surface of the sample with an angle of 45° while also the detector is located under the same angle to the sample. The diameters of the metal structures on the investigated sample vary between 40 nm and 2 µm with a fixed thickness of 35 nm for the chromium structures.

Besides the evaluation of the detection limit the prepared samples allow also to optimize the measurement setup due to focussing on structures with known shape. First measurements at BESSY have shown that the beam spot was not perfectly circular and had a second maximum, which results in a banana-like beam shape. The known shape of the metal structures helps to improve the setup of the beamline, as the optical components can be adjusted to result in an approximately circular beam profile. The overview image in Fig. 3 shows that the intensity of the XRF signal decreases clearly with the size of the metal particle.

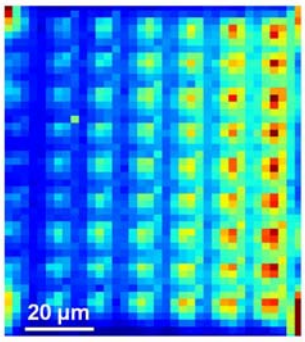

Figure 3: XRF measurement: Overview scanning of an array of chromium structures with different sizes (increasing particle sizes from left to right).

The detectable chromium spots using standard measurement conditions in step size (3 µm) and measuring time (1 s per step) correspond to a sphere with a radius of 150 nm. Combining oversampling (step size 500 nm) and extended measurement time (2 s) allows the detection of even smaller chromium structures down to spheres with 100 nm radius.

While the detection limit of the µSpot beamline at BESSY II may be critical for small precipitates, the main advantage is that relatively large areas in the range of a few hundred microns can be scanned by XRF. This allows a good pre-characterization of samples for further XRF measurements at other synchrotron radiation facilities or the investigation of highly contaminated material. Additionally, XANES measurements could be performed at this beamline.

ESRF

Secondly, the results at beamline ID22N at ESRF in Grenoble, France, will be discussed. The beam (FWHM: 200 nm) hits the sample surface perpendicular while the detector is located in a 45° angle to the sample in this measurement setup. Chromium structures with diameters in the range of 25 to 400 nm and a thickness of 30 nm were fabricated on a silicon wafer and are investigated by XRF.

Due to limited beamtime only the detection limit in case of standard measurement conditions (step size: 100 nm, 0.1 s per step) could be determined. This results in the detection of metal spheres in the range of 40 nm in radius.

Additionally, three chromium particles which were arranged in a triangular shape with varying distances were investigated. It was found that metal particles within a distance of 100 nm or larger can be separately detected in case of oversampling by step sizes of 50 nm (Fig. 4).

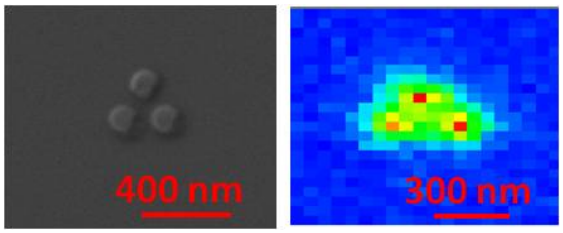

Figure 4: Scanning electron microscopy image (left) of arranged chromium structure on a FZ-Si wafer and the corresponding XRF measurement (right).

APS

It was assumed that the beamline 2-ID-D at APS in Argonne, USA allows the detection of even smaller particles than at ESRF. Therefore, the design of the E-beam writing pattern was adjusted again and smaller particles down to 15 nm in diameter and a thickness of 12 nm were fabricated.

The incident beam hits the sample surface at an angle of 20° while the detector is perpendicular to the beam. FWHM of the incident beam is below 200 nm.

Due to the destruction of the Chromium sample during the lift off process, the sample with Cu structures was used for this XRF analysis. At standard measurement conditions (step size: 100 nm, 1 s per step) even the smallest Cu structures with an equivalent radius of a sphere of 8 nm were detected and still result in a fluorescence signal which is a factor 2 higher than the background signal. Unfortunately, the spatial resolution of the used E-beam resist does not allow the fabrication of smaller metal structures.

5 SUMMARY

The detection limit of µXRF varies for the different synchrotron radiation facilities due to the different beamline setups and measurement conditions. While even the smallest metal structures corresponding to a sphere with a radius of 8 nm were detected by µXRF at APS in Argonne, USA, only structures in the range of 100 nm in radius could be detected at BESSY II in Berlin, Germany.

6 ACKNOWLEDGEMENT

We like to thank M. Hagner for assistance during sample preparation, as well as I. Zizak at BESSY II, G. Martinez-Criado at ESRF, B. Lai at APS and D. Fenning (MIT) for their help during µXRF measurements. The underlying projects of parts of this report were supported with funding of the Ministry of Science, Research and the Arts of Baden-Württemberg, Germany as well as the German BMU in the frame of the SolarFocus project (0327650H). The content of this publication is the responsibility of the authors.

7 REFERENCES

[1] J. Junge, A. Herguth, S. Seren, G. Hahn, *Reducing the impact of metal impurities in block-cast mc silicon*, Proc. 24th EU PVSEC, Hamburg 2009, 1131.

[2] T. Buonassisi, A. A. Istratov, M. Heuer, M.A. Marcus, R. Jonczyk, J. Isenberg, B. Lai, Z. Cai, S. Heald, W. Warta, R. Schindler, G. Willeke, and E.R. Weber, *Synchrotron-based investigations of the nature and impact of iron contamination in multicrystalline silicon solar cells*, J. Appl Phys 97 (2005) 074901.

[3] O.F. Vyvenko, T. Buonassisi, A.A. Istratov, E.R. Weber, *X-ray beam induced current/microprobe x-ray fluorescence: synchrotron radiation based x-ray microprobe techniques for analysis of the recombination activity and chemical nature of metal impurities in silicon*, J. Phys: Condens. Matter 16 (2004) 141.

[4] S. Hudelson, S. Bernardis, Y.S. Lee, K. Hartman, M. Bertoni, B. Newman, M.A. Marcus, B. Lai, S. Vogt, Z. Cai, T. Buonassisi, *Mitigating the "iron problem" in crystalline silicon solar cells*, Proc. 23rd EU PVSEC, Valencia 2008, 963.

[5] M.I. Bertoni, S. Hudelson, B.K. Newman, D.P. Fenning, H.F.W. Dekkers, E. Cornagliotti, A. Zuschlag, G. Micard, G. Hahn, G. Coletti, B. Lai, T. Buonassisi, *Influence of defect type on hydrogen passivation efficacy in multicrystalline silicon solar cells*, Progr. Photovolt: Res. Appl. 19 (2011), 187.

[6] A. Zuschlag, S. Ohl, J. Bernhard, H. Morhenn, J. Ebser, J. Junge, S. Seren, G. Hahn, *µXRF investigations on the influence of solar cell processing steps on iron and copper precipitates in multicrystalline silicon*, Proc. 35th IEEE PVSC, Honolulu 2010, 347.

[7] D.P. Fenning, J. Hofstetter, M.I. Bertoni, J.F. Lelièvre, C. del Cañizo, T. Buonassisi, *Synchrotron-based microanalysis of iron distribution after thermal processing and predictive modeling of resulting solar cell efficiency*, Proc. 35th IEEE PVSC, Honolulu 2010, 430.

[8] T. Buonassisi, A.A. Istratov, M.D. Pickett, M.A. Marcus, G. Hahn, S. Riepe, J. Isenberg, W. Warta, G. Willeke, T.F. Ciszek, E.R. Weber, *Quantifying the effect of metal-rich precipitates on minority carrier diffusion length in multicrystalline silicon using synchrotron-based spectrally-resolved X-ray beam induced current*, Appl. Phys. Lett. 87 (2005) 044101.

[9] P. Gundel, G. Martinez-Criado, M.C. Schubert, J.A. Sans, W. Kwapil, W. Warta, E.R. Weber, *X-ray excited optical luminescence from crystalline silicon*, Phys. Stat. Sol. RRL 7-8 (2009) 275.